Water Air Soil Pollut (2024) 235:46
https://doi.org/10.1007/s11270-023-06851-2

4-Acyl Pyrazolone–Modified Silica as a New Sorbent for Selective Solid-Liquid Extraction of Pb (II)

Purva Kachhi · Rajendrasinh N. Jadeja

Received: 21 September 2023 / Accepted: 14 December 2023 / Published online: 29 December 2023

Abstract A Schiff base reaction was used to create a newly constructed silica hybrid material (SiNP-L_3) by functionalizing (4-chlorophenyl) [5-hydroxy-3-methyl-1-(4-methylphenyl)-1*H*-pyrazol-4-yl] methanone over modified silica. To show the successful addition of Schiff base groups, scanning electron microscopy, the Fourier transformation of infrared spectroscopy, elemental examination, BET surface measurement, Barrett-Joyner-Halenda pore dimension, solid state ^{13}C-NMR, powder XRD, and thermogravimetry measurements were done on the prepared sorbent, which was used to selectively remove lead in the aqueous media. Batch studies were used to examine the effects of interaction duration, starting concentration, pH levels, and sorbent dosage on the degree of sorption of lead (mg/g). Langmuir adsorption isotherm and pseudo-second-order (PSO) kinetic model fit best to the obtained data with R^2 values of 0.98 for both which shows the major possibility of chemisorption. The positive values of ΔS° and ΔH° reflect the endothermic behavior of the adsorption technique, whereas a downward trend in Gibbs free energy (ΔG°) with rising temperature demonstrates the spontaneous character of the adsorption process. Additionally, the newly created material stimulates easy recycling up to five times in sequence without compromising the extraction percentage and shows high selectivity for Pb (II) having an adsorption capacity of 16.8 mg g^{-1}.

Keywords Adsorption · Adsorption capacity · Efficiency · Isotherm · Kinetics · Silica

1 Introduction

Due to their propensity to gather in animals and plants and their toxicity to aquatic life, humans, and the ecosystem, heavy metal ions have been a major worry among many industrial branches related to environmental pollution. Pb (II) stands out as one of the most problematic heavy metals among all the others since it has a negative impact on the health of humans as well as animals and prevents water bodies from purifying themselves from it (L. Li et al., 2020). Lead is used in a variety of industrial processes, including those that create alloys, electrical products, chemical catalysis, polished metal surfaces, and batteries. Because lead has been found to cause damage to the brain in children even at low amounts, lead is at the top of the list among environmental dangers (Mishra & Patel, 2009). In addition to anemia, brain damage, mental deficiencies, and behavioral issues

Supplementary Information The online version contains supplementary material available at https://doi.org/10.1007/s11270-023-06851-2.

P. Kachhi · R. N. Jadeja (✉)
Department of Chemistry, Faculty of Science,
The Maharaja Sayajirao University of Baroda,
Vadodara 390002, India
e-mail: rajendra_jadeja@yahoo.com

in people, it also kills plants and animals. In skeletal tissues, lead replaces calcium and builds up and lead within drinking water has been linked to several major health issues, including those that can be fatal in some circumstances (Low et al., 2000). So, acceptable limits have been set at 0.01 mg L^{-1} by the World Health Organization (WHO) and 0.05 mg L^{-1} by the US Environmental Protection Agency (USEPA) (Li et al., 2020).

Although these techniques have negative non-economic effects, it is said that liquid-based extraction (Nasu et al., 1997), Coprecipitation (Soylak & Erdogan, 2006), exchange of ions (Tao & Fang, 1998), adsorption, membrane filtration (Bessbousse et al., 2008), resin chelation (Atia et al., 2005), and electrochemical technologies are efficient at eliminating heavy metal ions from water bodies. On the other hand, improved enrichment factors, easy ease of use, protection with reference to noxious substances, great selectivity, decreased cost, quick recovery, and versatility to integrate it with many advanced detection strategies are only a few of the major advantages of solid-phase extraction (SPE) (Zhang et al., 2010). In fact, the SPE is regarded as a potent method for the extraction and enhancement of a number of inorganic and organic analytes (Bacalum et al., 2011; Radi et al., 2019).

Modified inorganic-organic composites have recently been used extensively as affordable adsorbents to extract heavy metal ions from water bodies due to their interesting qualities, including significant linking preferences, selectivity, excellent adsorption rates with regard to heavy metal ions, enormous areas of surface, and superior thermodynamic, chemical, and mechanical stabilities (Ahmed et al., 2020). There are a variety of modern natural and manufactured solid supports that, with just a few modifications or chemical alterations, can become effective sorbents. Although clays are a natural choice, synthesized silicas may have greater capabilities for significant surface modification to enhance adsorption sites and selectivity (Radi et al., 2014).

Silica has pore diameters that vary from microporous to mesoporous (5 to 500 A^0) and huge surface areas (>600 m^2 g^{-1}). It comprises of siloxane (Si-O-Si) and silanol (Si-OH), two different types of functional groups. As an outcome, silica gel modification can take place as a result of a reaction involving a specific molecule that reacts either with siloxane (nucleophilic substitution at the Si) or silanol (direct interaction with the hydroxyl group) functionalities (Price et al., 2000). Research has revealed three primary techniques for attaching functional groups to silica surfaces: (i) by means of an interaction between organic or organosilane molecules and the functionalities of silica surfaces; (ii) first, the silica surface is chlorinated, and then the Si-Cl is reacted with the proper functional molecule or reactant; (iii) functional groups are included using the sol-gel technique, and then post modification is applied as needed (Price et al., 2000). However, it has been shown that the stable azomethine group, also known as an imine or Schiff base, has a significant impact on stabilizing metal complexes because it can act as a good interaction site for plenty of transition metals, resulting in steady coordination complexes (Ahmed et al., 2020). There have been several reports of extractants in this context that possess Schiff base functionality grafted on a porous silica substrate (Al-Wasidi et al., 2022a; Al-Wasidi et al., 2022b; Amarasekara et al., 2009a; Koorepazan Moftakhar et al., 2016; Radi et al., 2013; Radi et al., 2014; Radi et al., 2019; Song et al., 2023; Tighadouini et al., 2017; Zheng et al., 2021).

Although many literature reports are there based on excellent chelating ability and useful applications of 4-Acyl pyrazolone ligands, very few reports are there which include 4-acyl pyrazolone functionality grafted on solid support utilized for extraction of heavy metal ions (Pratiwi et al., 2017; Tong Akama & Tanaka, 1990), out of which some focuses on lanthanide extraction only (Amarasekara et al., 2009a; Amarasekara et al., 2009b; Tong Akama & Tanaka, 1990).

The aim of the present work is to develop an acyl pyrazolone containing Schiff base ligand anchored on porous silica substrate for the selective solid-liquid extraction of lead (II) since acyl pyrazolones are an intriguing family of beta-diketones with outstanding metal chelating abilities. To create a very effective and focused sorbent for the targeted extraction of Pb (II), we have here used a porous, high surface area silica support. Here, we have used the first method out of the three mentioned above for modification of the silica surface which involves the reaction of 3-aminopropyl trimethoxy silane with surface silanol (-OH) groups of silica. The conversion to a Schiff base derivative is an attractive modification of the 4-acyl pyrazolone system, which replaces one oxygen

atom with a nitrogen donor atom and provides a convenient anchoring point to the ligand (Amarasekara et al., 2009b). An entirely new substance created by grafting (4-chlorophenyl) [5-hydroxy-3-methyl-1-(4-methylphenyl)-1*H*-pyrazol-4-yl] methanone can serve as a chelating arm on functionalized porous silica in an N, O-bidentate way creating six-membered chelating rings. To make it easier for the receiver and metal ion to make contact, this ligand was immobilized on silica gel using a long arm spacer (Radi et al., 2014). The solid-phase ^{13}C-NMR, nitrogen adsorption-desorption isotherm, Fourier transformation of infrared spectroscopy, elemental examination, thermogravimetry measurements, BET surface area, BJH pore size measurement, scanning electron microscopy (SEM), and powder XRD studies were used to thoroughly evaluate the new chelating material. In the presence of other heavy metal ions, including Cd (II), Cu (II), Cr (II), Ni (II), and Zn (II), as well as alkali and alkaline earth metals, we evaluated its selectivity for adsorption of Pb (II) in aqueous samples using an atomic absorption spectrophotometer (AAS).

2 Experimental

2.1 General Information

All solvents and other compounds were of analytical standard and utilized without additional processing (purity > 99.5%, Aldrich, SRL, and Loba Chemie). Silica gel was heated at 120 °C for a day to activate it before use (Loba Chemie, Mumbai, Maharashtra). The particle size range was 70–230 mesh, and the median pore diameter was 60 Å. Without any prior purification, the silylating agent 3-aminopropyltrimethoxtsilane (SRL, Mumbai, India) was utilized. Analytical grade $Pb(NO_3)_2$ was used for the lead extraction study.

2.2 Synthesis of 3-Aminopropylsilica ($SiNH_2$)

The interaction between the silylating substance and the silanol moieties on the exterior of silica was the first stage in the preparation. The previously described process was followed in doing this (Radi et al., 2014). Under a nitrogen environment, activated silica gel (10 g, SiO_2) was refluxed and physically agitated for 2 h in dried toluene (60 mL). Dropwise additions of 3-aminopropyltrimethoxysilane (4 mL) were made to this suspension, and the mixture was then maintained at reflux for a day. The filtered material was then cleaned with ethyl alcohol and toluene. The excess silylating agent was subsequently removed using a 12-h Soxhlet extraction with an equal mixture of ethanol and dichloromethane. The resulting product ($SiNH_2$, 12.5g) was then dried under reduced pressure for 8 h at 100°C. $SiNH_2$, the modified silica gel, was vacuum-dried at ambient temperature. The amine group coated on the surface of silica (1.6 mmol/g) was identified by reacting with an excess of 4×10^{-2} mol/L aqueous HCl, following a titration with 4×10^{-2} mol/L aqueous NaOH and utilizing phenolphthalein as an indicator.

2.3 Synthesis of (4-Chlorophenyl) [5-Hydroxy-3-Methyl-1-(4-Methylphenyl)-1H-Pyrazol-4-yl] Methanone **(L_3)**

Acyl pyrazolone ligand (L_3) was prepared according to a previously published literature by our research group (Shaikh et al., 2020; Shaikh et al., 2021) which was according to Jensen's method (Jensen, 1959). (1) FT-IR (KBr, cm^{-1}): 1552 (C=N, cyclic), 1592 (C=O, 4-chloro benzoyl group), and 1600 (m) (C=O, Pyrazolone ring); (2) ^{1}H-NMR ($CDCl_3$, ppm, 400 MHz): 2.13 (s, 3H), 2.41 (s, 3H), 7.29 (d, J = 8.4Hz, 2H), 7.51 (d, J = 8.4Hz, 2H), 7.61 (d, J = 8.4Hz, 2H), and 7.73 (d, J = 8.4Hz, 2H). Fig. S1 and S2 show ^{1}H-NMR and FT-IR spectra for ligand L_3, respectively.

2.4 Synthesis of (4-Chlorophenyl) [5-Hydroxy-3-Methyl-1-(4-Methylphenyl)-1H-Pyrazol-4-yl] Methanone Substituted Silica (SiNP-L_3)

L_3 ligand (8.0 g) and aminopropylsilica-$SiNH_2$ (5.0 g) were mixed in 60 mL of dry methanol and agitated at 70–80°C for 48 h to generate SiNP-L_3. Following filtering, the solid material was subjected to a 12-h Soxhlet treatment using acetonitrile, methyl alcohol, and dichloromethane, respectively. The product (SiNP-L_3, 5.4g) was then vacuum-dried for 24 h at 70°C.

2.5 Batch Experiment Studies

The batch approach was used to investigate how the initial concentration, adsorbent dose, pH, and duration of stirring affected the uptake of Pb (II) by the

prepared sorbent SiNP-L_3. By agitating 20 mg of the modified silica gel with 10 mL of a lead solution with concentrations ranging from 50 to 250 mg/L, for different time intervals (1, 3, 5, 15, 30 min and 1, 2, and 24 h) and different pH values (1–8), the modified silica gel was brought to equilibrium. Compared to the capacity for sorption, the proportion of metal ions was excessive. 500 mg/L of aqueous stock solution of lead (II) ions was prepared by dissolving 0.799 mg of lead (II) nitrate ($Pb(NO_3)_2$) in 1 L of double distilled water. It was diluted to make solutions of 50, 100, 150, 200, 250 mg/L as required for optimization studies. The stock solution was stored in the refrigerator and was used for 45 days.

Atomic absorption measurements were used to estimate the lead ion concentration. The following algorithms were used to compute the adsorption amount (Q_e, mg/g) and extraction (%) (Irfan et al., 2022).

$$Extraction(\%) = \left\{\left(C_o - C_e\right)/C_o\right\} \times 100 \quad (1)$$

$$Q_e(mg/g) - \left\{\left(C_o - C_e\right)/M\right\} \times V \quad (2)$$

where the metal ion amount on the adsorbent at equilibrium is indicated by Q_e (mg/g), V is the abbreviation for the aqueous solution's volume (l), C_0 represents the metal ion's starting amount (mg/L), the equilibrium concentration of the metal ion in solution is expressed by C_e (mg/L), and M is the weight (g) of the adsorbent utilized, SiNP-L_3. The analyses were done in triplicate for each sample, and the mean outcomes are shown.

2.6 Physical Measurements

Atomic absorption measurements were made using a Perkin Elmer AAcle 500 Atomic Absorption Spectrometer to identify the quantity of adsorbed metal ions. Elemental analyses were performed by using Elementar Analysensysteme (GmbH, Germany by Unicube) at the Sophisticated Instrumentation Center for applied research and testing (SICART, Anand, Gujarat). At room temperature, FT-IR scans of SiNP-L_3 as KBr discs were captured using a PerkinElmer IR spectrophotometer. SEM images were obtained on Hitachi SU1510 VP-SEM (Department of Geology, MSU, Baroda). With the nitrogen environment maintained during the measurement, the mass loss calculations were carried out in the TG-DTA 6300 INCARP EXSTAR 6000 using a temperature rise of 10 °C/min in the temperature interval between 25 and 600 °C. The ^{13}C-NMR spectrum of the solid-state was obtained with a CP MAS ECZR series 600 MHz instrument (JEOL, Japan). Powder XRD was carried out using Rigaku smart lab SE 3 kW equipped with Cu-Kα(0.154nm) source (Department of Applied Physics, MSU, Baroda). FE-SEM analysis of the vacuum-dried Pb (II) adsorbed SiNP-L_3-Ads was recorded by the model JSM7600F (Jeol) combined with an energy dispersive spectrometer (EDS). The precise surface area was calculated utilizing the BET equation. After the material had been immersed in a steady flow of dry nitrogen, the nitrogen adsorption-desorption was measured using a Micrometrics ASAP 2010 device at a temperature of 196 °C.

3 Results and Discussion

3.1 Sorbent Synthesis

Figure 1 provides a summary of the process for creating the novel chelating substance, SiNP-L_3. In order to generate the sorbent (SiNP-L_3), 3-aminopropyltrimethoxysilane was used to initially modify the surface of the activated silica gel through a reaction with exterior silanol groups in dry toluene as a solvent. In a dry methanol, acyl pyrazolone

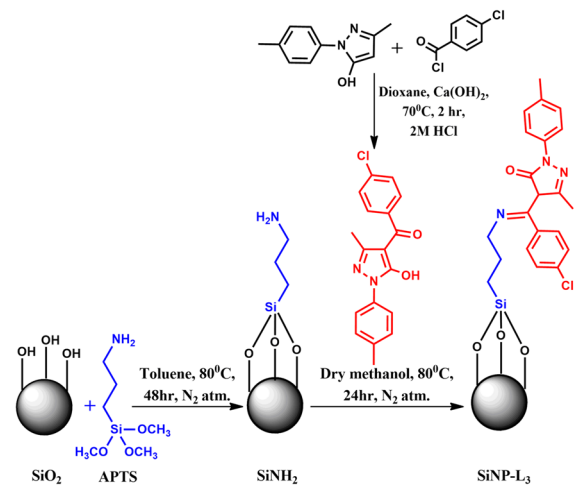

Fig. 1 Synthetic procedure of new chelating material SiNP-L_3

Fig. 2 Physical appearance of **a** free silica gel (SiO_2), **b** $SiNH_2$, **c** SiNP-L_3

Table 1 Elemental analysis of free silica gel (SiO_2), $SiNH_2$, and SiNP-L_3

Material	Elemental analysis (%)		
	C	H	N
SiO_2	-	-	-
$SiNH_2$	7.14	2.594	2.17
SiNP-L_3	14.06	2.664	2.82

ligand-L_3 was then reacted with 3-aminopropyl silica ($SiNH_2$), and imine functionality was introduced. Figure 2

3.2 Sorbent Characterization

3.2.1 Elemental Analysis

It is feasible to identify and emphasize the added organic functionalities on the exterior of silica owing to the elemental composition of aminopropyl-grafted silica $SiNH_2$ and SiNP-L_3 which contains carbon and nitrogen that were absent in the beginning activated silica. It is apparent that the 3-aminopropyl chain has successfully grafted on the surface of silica by replacing three silanol groups as suggested by the microanalysis results (%C =7.14%, %N =2.17 and %H = 2.594) and C/N ratio from practically and theoretically obtained formulas, which is given as supplementary data (Table S1). The percentage of C, N, and H in the final sorbent SiNP-L_3 has increased (%C = 14.06, %N = 2.82, and %H = 2.664) as given in Table 1, indicating that the acyl pyrazolone units were successfully immobilized on the silica gel surface (El Abiad et al., 2017).

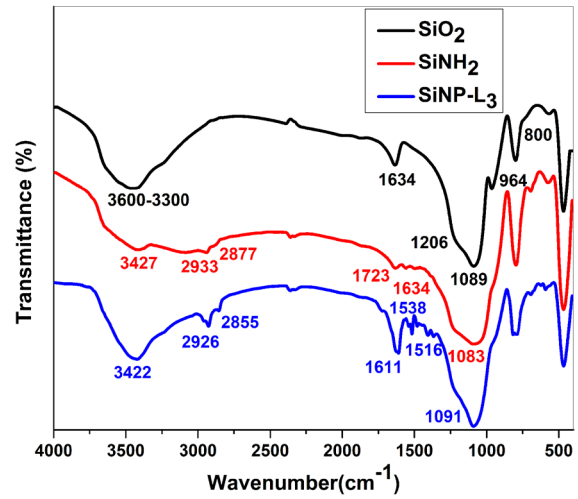

Fig. 3 Fourier transform infrared spectrum of free silica (SiO_2), $SiNH_2$, and SiNP-L_3

3.2.2 FT-IR Analysis

Figure 3 represents the FT-IR bands of free silica gel (SiO_2), $SiNH_2$, and ligand-L_3 grafted silica (SiNP-L_3). Appearance of some new bands and increase or decrease in intensity of others confirms the specific functionalization of silica surface. In the case of free silica, the O-H stretching and bending of the exterior silanol moieties and physically retained water (H_2O) are responsible for the broadband between 3600 and 3300 cm^{-1} and the band at 1634 cm^{-1}, respectively. Specific bands at 1089 cm^{-1} and 964 cm^{-1} are linked to Si-O-Si pulling and Si-O vibrations of exterior silanol groups, respectively (Han et al., 2005). In the FT-IR spectra of $SiNH_2$, a new band corresponding to the CH stretching of the propyl chain developed at

2933 and 2877 cm^{-1} in contrast to free silica (Jiang et al., 2007). A band at 964 cm^{-1} vanished in comparison to free silica, while additional bands at 1723 cm^{-1} and 1634 cm^{-1} emerged as a result of the free amine group's -NH bending (Radi et al., 2014). SiNP-L_3 differs from $SiNH_2$ in that the reaction of primary amine (-NH_2) causes the adsorption band at 1634 cm^{-1} to vanish and a new characteristic band appears around 1500 cm^{-1} specifically at 1516 cm^{-1} and 1538 cm^{-1} as a result of the -C=N- vibrations of the cyclic and acyclic imine functionalities of Schiff base acyl pyrazolone, which supports the precise anchoring of the organic molecule onto the silica surface. Moreover, the C=O motions of the amide group located within the acyl pyrazolone framework can be offered a substantial adsorption band at 1611cm^{-1} (Amarasekara et al., 2009a; Amarasekara et al., 2009b). Fig. S3–S5 depict the FT-IR bands of all three materials.

3.2.3 *Thermogravimetry Measurements and Thermal Stability*

To determine the organic content and to assess the possible thermal strength of the created sorbent SiNP-L_3, TG analysis was performed. As shown in Fig. 4, the thermogravimetric curves for all surfaces allowed the establishment of the data on thermal stability and the confirmation of the quantity of the chemicals immobilized. The fact that the created materials degrade between 131 and 550°C confirmed its high thermal stability. Due to physically captured water and the combination of the unbound silanol groups into siloxane (Si-O-Si) functionality, there was a first mass loss of 3.8% between rt and 110°C and a second mass loss of 2.01% within 110°C and 550°C (Sales & Airoldi, 2005), respectively, were the important features of free silica gel (SiO_2). Again, $SiNH_2$ shows two specific mass loss regions: (1) the silanol moisture retention that is still available due to the use of these molecules in the binding reaction initially causes a slight mass reduction of 22.2% in the temperature range of rt to 180 °C and (2) a considerable mass loss increase of 11.6% was seen during the second step between 208 and 550°C as a result of the organic content that was added to the outer layer during grafting, and it continued after that. Two noticeable mass loss regions were observed for final sorbent SiNP-L_3. According to the previous elucidation, the initial mass reduction of 5.1% within rt to 180.37°C is attributed to consumed water, and the second mass loss of 14.82% between 200 and 550°C which also shows sudden decrease after 550°C is assigned to the acylpyrazolone units anchored on the outer layer and the combination of the remained silyl alcohol groups (Tighadouini et al., 2017). The increase in organic chain that is covalently linked to the silica surface and the rising amount of anchoring organic functionalities are consistent with the rise in mass loss, as represented in Fig. S8–S10.

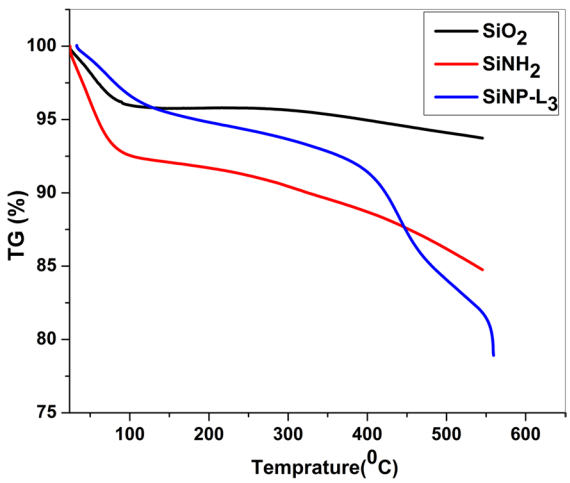

Fig. 4 Thermogravimetric analysis of free silica (SiO_2), $SiNH_2$, and SiNP-L_3

3.2.4 *Solid-State ^{13}C-NMR*

^{13}C NMR peaks in the stationary state can be utilized to detect significant characteristics of the binding of suspended groups on the inorganic skeleton of the blend produced, as shown in Fig. 5. The signals for propyl skeleton Si-CH_2, -CH_2-, and N-CH_2 observed at δ = 9.72, 21.72, and 42.55 ppm, respectively, in NMR spectra of $SiNH_2$. The most downfield signal at 165.28 is due to imine C and other signals at 146.58, 136.59, 128.61, 117.77, 99.25, 51.26, and 12.95 ppm region occurred due to the anchoring of the L_3 ligand; these signals demonstrate the alteration of the support surface and are indicative of the groups found in the framework of the pyrazolone derivative (Tighadouini et al., 2017). Fig. S11 and Fig. S12 show ^{13}C-NMR spectra of $SiNH_2$ and SiNP-L_3, respectively.

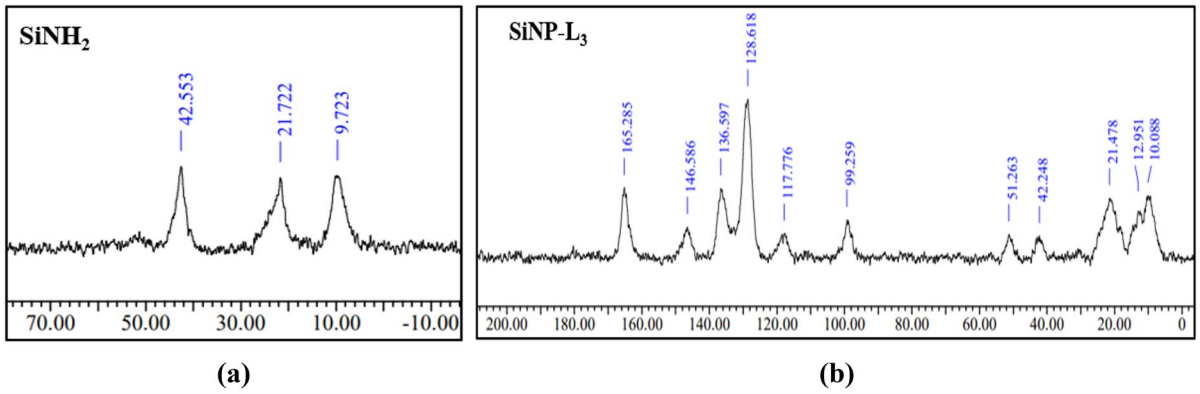

Fig. 5 ^{13}**C** NMR spectra of **a** 3-aminopropyl grafted silica ($SiNH_2$) and **b** acylpyrazolone-grafted silica ($SiNP\text{-}L_3$)

3.2.5 Chemical Stability

To illustrate the chemical sustainability of the final sorbent $SiNP\text{-}L_3$, several acidic and buffered mixtures (pH 1–7) were utilized. Even after 24 h of interaction, there was no evident alteration in the material's extraction properties. We have measured its weight and investigated its extraction capacity by doing extraction experiments maintaining the optimized condition using the AAS (atomic absorption spectrophotometer) instrument. Also, we have taken its FT-IR spectra (in the case of both acidic and basic pH) to confirm structural changes if any, but there was no change. S6 and S7 depict FT-IR spectra of prepared adsorbent $SiNP\text{-}L_3$ after 24 h of interaction with acidic media (pH=2) and basic media (pH=10). The pendant group is most likely responsible for the connected organofunctional group's high level of stability. Because prolonged chains lack an effective grip that can undergo Si cation b-elimination, the breakage of the Si-C bond in a mineral acid medium was shown to be prevented when the span of the hydrocarbon link was more than two methylene groups (Mureseanu et al., 2010; Roumeliotis et al., 1983).

3.3 Surface Analysis

3.3.1 Scanning Electron Micrographs

In order to identify alterations to the surface morphology of free silica and chemically transformed silicas, SEM analyses were performed on all four materials. SEM images of free silica gel, $SiNH_2$, $SiNP\text{-}L_3$, and Pb (II) adsorbed material depicted as $SiNP\text{-}L_3$-ads shown in Fig. 6 were taken at 100–1000 magnifications. Due to the higher number of organic components than the initial non-functionalized silica, which was smooth, the external layer of functionalized particles becomes rougher and has a tendency to partially agglomerate. That organic moieties were successfully caught on the surface is confirmed by the roughness. It is well-recognized that a rough surface typically offers favorable characteristics for usage as an adsorbent. It was clear that the organic functionalities were spread throughout the exterior of the product $SiNP\text{-}L_3$, which had a uniformly rough surface due to the attachment of a big pyrazolone ligand (Tighadouini et al., 2017). Furthermore, the exterior of lead-adsorbed material ($SiNP\text{-}L_3$-ads) features a regular triangle pattern covering the entire surface, which can be attributed to the consistent complex formation of Pb (II) with binding units anchored on the surface.

3.3.2 FE-SEM and EDX Analysis

The elemental composition and surface morphology of synthesized adsorbent $SiNP\text{-}L_3$ was confirmed using field emission scanning electron microscope coupled with energy dispersive spectrometer. This technique is of great importance for analyzing surface morphology and composition. The morphology of Pb (II) loaded adsorbent is presented in Fig. 7. According to EDS analysis of $SiNP\text{-}L_3$-ads, the carbon and oxygen dominate the composition, and the presence of nitrogen confirms the imine linkage with silica surface (Yadav et al., 2022).

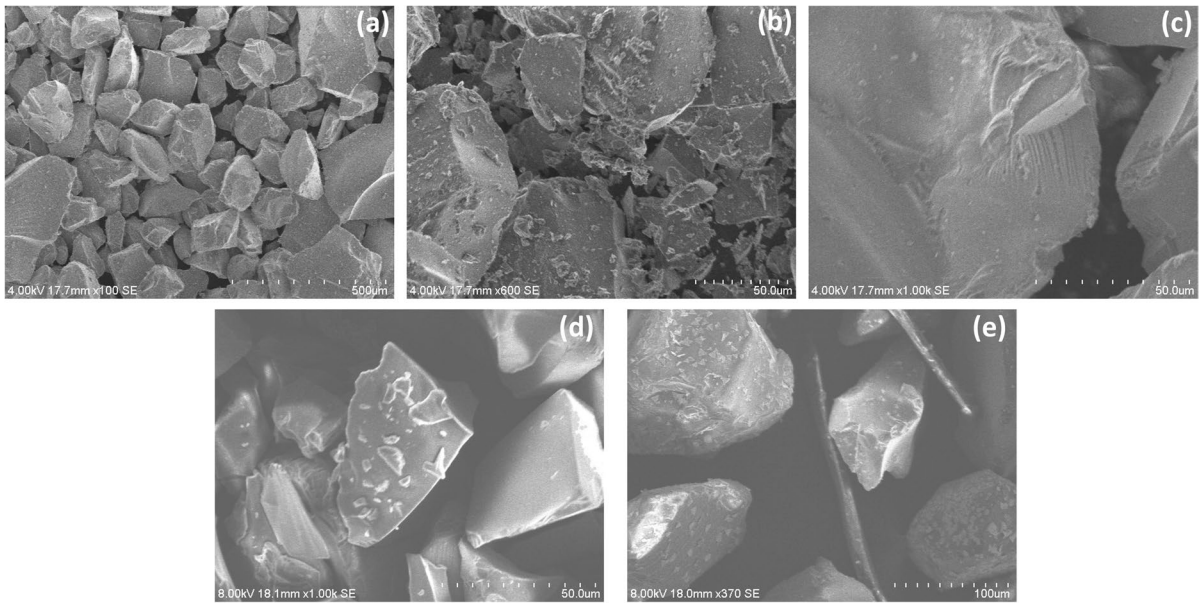

Fig. 6 SEM images of a unmodified silica (SiO_2), b $SiNH_2$, *c* and *d* SiNP-L_3, and *e* SiNP-L_3-ads

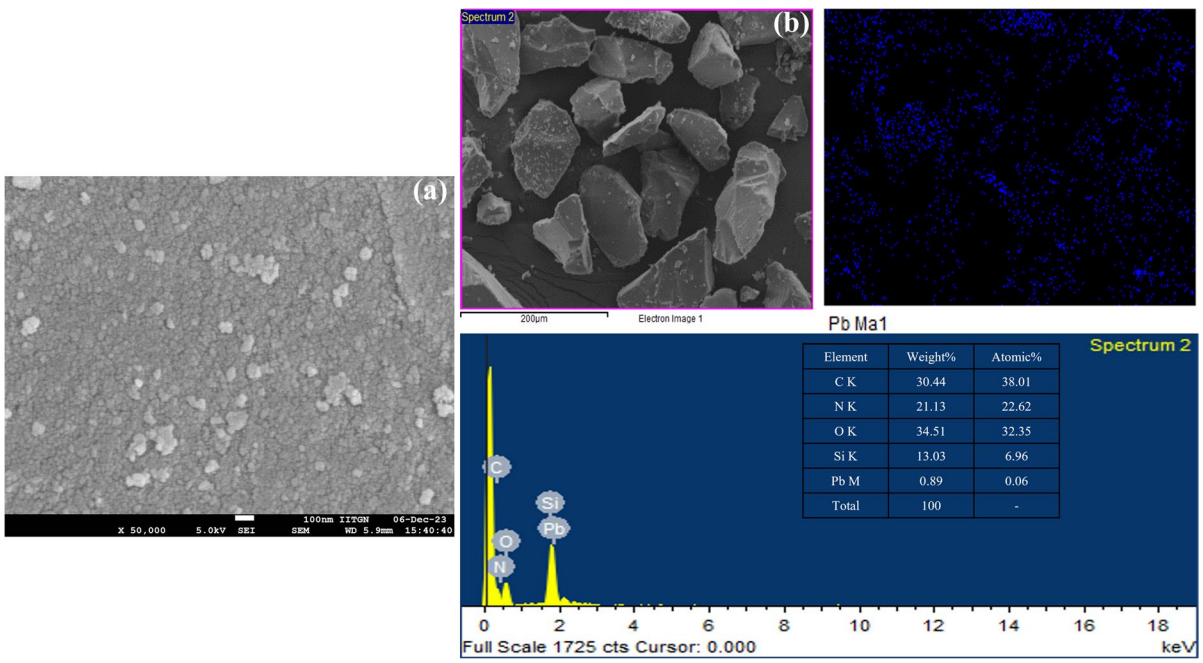

Fig. 7 **a** FE-SEM analysis and **b** EDX analysis of Pb (II) adsorbed material (SiNP-L_3-ads)

3.3.3 Powder XRD

Finally, the X-ray diffraction was used to study the inner skeleton of the sorbent and to compare it with that of the non-functionalized silica. The XRD patterns in Fig. 8 show two distinct peaks indexed at around 100 and 110, demonstrating that the materials maintained their mesoporous structure afterward

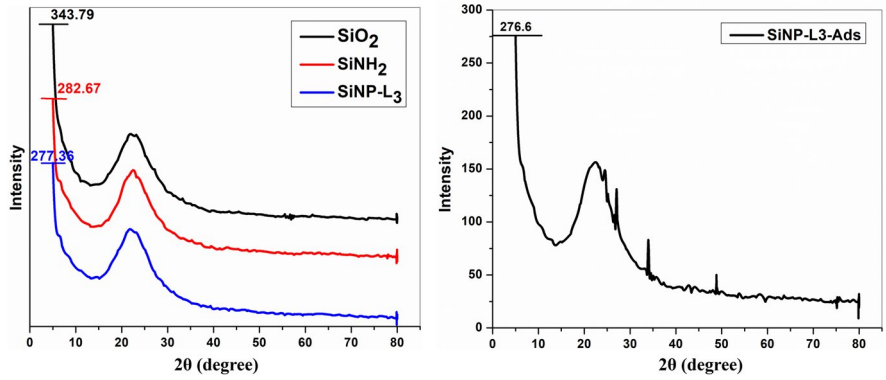

Fig. 8 X-ray diffraction patterns of SiO_2, $SiNH_2$, SiNP-L_3, and SiNP-L_3-ads

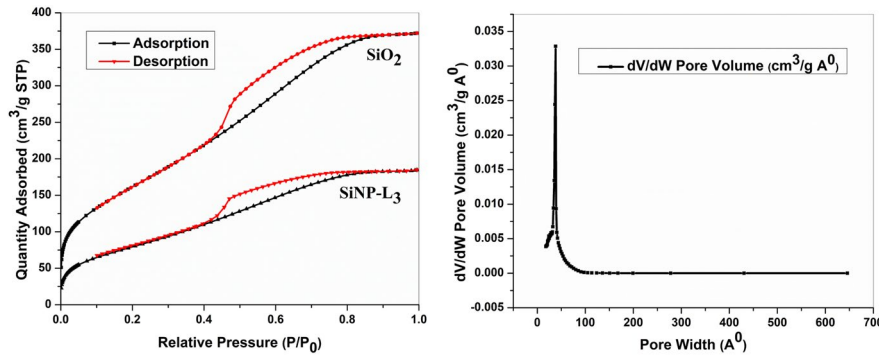

Fig. 9 Nitrogen adsorption-desorption isotherm and plot of pore diameter vs pore volume of SiNP-L_3

modification without experiencing any considerable change. Furthermore, a well-organized material type is indicated by the distinctive broad peak at 2Θ (around 5°), which is in accordance with the pore family (100). Since there are no peaks associated with a crystalline phase, the other little broad peak (110), which is at a high 2Θ angle (at about 23°), is typical of amorphous silica. The loss of the long-range porosity order during the functionalization process can be explained by the drop in intensity at (100), which also shows that the mesoporous channels were where the functionalization took place most frequently (Miao et al., 2009; Radi et al., 2018). Also, the powder XRD pattern of Pb (II) adsorbed material SiNP-L_3 shows the change in structure and incorporates some new sharp peaks which can be due to the complex formation with Pb (II).

3.3.4 BET Surface Area and BJH Pore Size Analysis

To demonstrate the porosity alterations of the silica brought about by the introduction of the acylpyrazolone unit, we measured the exterior area

Table 2 Physical measurement values of surface area and pore volume of silica and its derivative SiNP-L_3

Substrate	Specific surface area (m^2/g)	Pore volume (cm^3/g)
Free silica	601.6	0.58
SiNP-L_3	298.2	0.28

S_{BET} (Brunauer-Emmett-Teller) (George & Stephen Brunauer, 1938), pore volumes, and pore dimensions of both silica and its derived product by employing nitrogen adsorption-desorption isotherms (Fig. 9) and by Barrett-Joyner-Halenda (BJH) pore diameter measurements. The density of the hooked moieties covalently bonded to the inorganic silica framework changes the surface's original characteristics. As seen in Table 2, as encapsulation proceeds, the original specific surface area S_{BET}, which was 601 m^2 g^{-1} and had a pore volume of 0.58 cm^3 g^{-1}, drops to 298 m^2 g^{-1} and a pore size of 0.28 cm^3 g^{-1}. Organic elements that may block nitrogen from reaching the silica base are the primary factor causing a decrease in S_{BET}

(Radi et al., 2014). Additionally, the nitrogen-induced adsorption-desorption isotherm for silica derivative in Fig. 9 demonstrates a considerable hysteresis for partial pressures $1> P/P_0 > 0.4$ and is categorized by the IUPAC as type IV (Miao et al., 2009; Sing & Williams, 2004) which suggested a capillary condensation of the mesoporous substrate (Zheng et al., 2021).

3.4 Solid-Liquid Adsorption of Lead (II) by SiNP-L_3

3.4.1 Effect of Starting Concentration (C_0)

In order to determine the ideal adsorbate concentration, solutions with Pb (II) concentrations of 50–250 mg/L were examined using an adsorbent dosage of 10 mg as shown in Fig. 10a. It was discovered that the sorbent capacity does not significantly increase as compared to concentration at concentrations greater than 50 mg/L.

3.4.2 Influence of Sorbent Dosage (mg)

The sorbent quantity ranged from 10 to 60 mg in a 10 ml solution having 50 mg/L of Pb (II) in order to optimize the quantity of sorbent needed for significant extraction of Pb (II) as presented in Fig. 10b. As we can see in Fig. 10b, if we increase the dose after 20 mg (30, 40, 50 mg, etc.), extraction capacity (mg/g) does not increase much compared to that in the case of changing the dose from 10 to 20 mg. Also, if we consider a dose of more than 50 mg, we have to compromise its extraction efficiency which will not be convenient. Thus, as the best sorption was shown to occur at a sorbent dose of 20 mg, we considered it as an optimum dose for further studies.

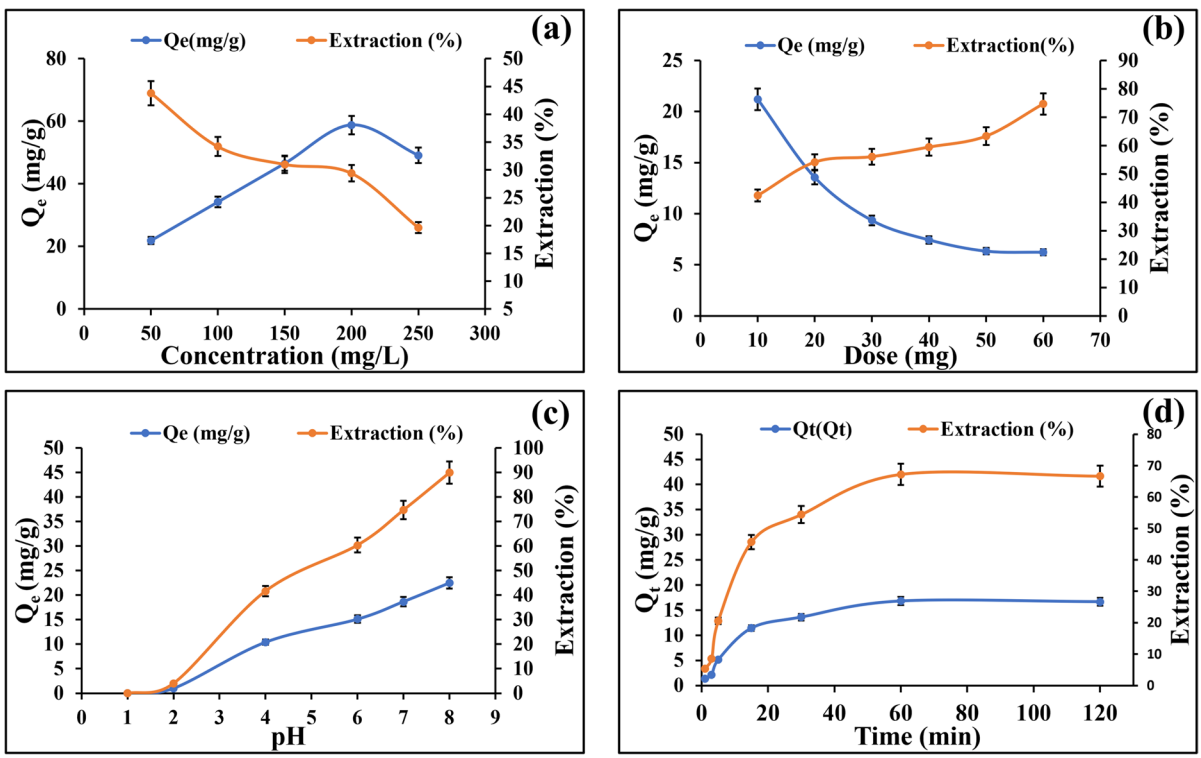

Fig. 10 **a** Effect of initial Pb^{2+} content on SiNP-L_3 adsorption capability and extraction efficiency at 25°C (10 ml, 20mg of sorbent, pH=5). **b** Influence of SiNP-L_3 amount on the percent elimination of Pb^{2+} from 10ml of 50 mg/L Pb^{+2} solution at pH=5. **c** Influence of pH on extraction efficiency of Pb^{2+} by SiNP-L_3 at 25°C (10 ml, 50 mg/L Pb^{+2}, 20 mg of sorbent). **d** Impact of interaction time on the adsorption capability and extraction efficiency of sorbent SiNP-L_3 (10 ml, 50 mg/L Pb^{+2}, 20 mg of sorbent, pH=6)

3.4.3 *Effect of pH*

It is widely acknowledged that the main factors that influence the metal ion binding to the chelate compounds, whether in solution or applied to solid supports, are the type, charge, dimensions (Myers, 1978; Pearson & Busch, 1963), form and interaction characteristics of the donor atoms, and the buffering conditions. These parameters have been extensively studied in both solution chemistry and in the solid-liquid extraction of specific metals by organic chelates anchored on the exterior of solid supports like silica gel, nanocomposites, or polymeric moieties. Thus, as one of the most important governing factors in such a procedure, we investigated the impact of the pH of the solution containing Pb (II) on the metal extraction capacity in order to assess the feasibility of the synthesized material SiNP-L_3 for Pb (II) separation and its bonding. pH range of 1–8 was used for the estimation of the adsorption qualities of SiNP-L_3 as shown in Fig. 10c. The findings show that the metal ion intake of the adsorbent varies significantly as the pH fluctuates. At lower pH levels, the consumption of Pb (II) ions by the altered silica SiNP-L_3 is minimal because the ligand must be almost entirely in its protonated form (Radi et al., 2014). The protonation weakens as the pH rises, enhancing the coordinate interaction and uptake of Pb (II) ions. It is challenging to tell if the lead (II) in Fig. 10c is adsorbed or hydrolyzed because lead ions get hydrolyzed at pH values higher than 6.5, which results in the formation of Pb (II) hydroxides: Pb $(OH)^+$ and Pb $(OH)_2$. So, pH=6 was the most suitable pH for the highest possible sorption of Pb (II). Also, we have determined the pH of the solution after the sorption study. We observed that pH of solution increases in case of acidic pH while pH of solution decreases in case of basic pH after sorption. This could be due to the fact that adsorbent will acquire positive charge on their surface in acidic pH due to the protonation of N and O donor atoms in the ligand (extraction (%) decreases), and this protonation becomes weak in basic pH (Extraction (%) increases).

3.4.4 *Effect of Contact Time and Adsorption Kinetics*

The duration of stirring required to achieve equilibrium conditions and the Pb (II) adsorption by the ligand L_3 functionalized silica gel is crucial. Batch experiment studies were used to examine the impact of interaction time on the uptake of Pb (II) by SiNP-L_3. The Pb (II) kinetic charts demonstrated that the sorption was fast, and a saturation point was reached after roughly 60 min of contact, as can be shown in Fig. 10d, but to examine the effect of extended time on the extraction percentage (%), the study was kept for 24 h, and the change was insignificant. The rapid Pb (II) ion adsorption demonstrates that the engaged donor atoms, oxygen and nitrogen, on the exterior of the improved silica gel are oriented in a manner that does not restrict their affordability, allowing for rapid contact with the Pb (II) ions in the solution. Rapid kinetics is extremely useful since it enables reduced reactor sizes while maintaining efficiency and economics.

Extraction kinetics is essential for practical applications, operation control, and design because it provides significant insights regarding the reaction route and the internal workings of the procedure of the uptake. Kinetics may now be used to explain the consumption of solutes by controlling the degree of adsorbate acceptance at the junction between solid and solution. As we are focusing on developing acyl pyrazolone–incorporated adsorbent material for extraction of heavy metal ions which was not reported before, in order to prove the exact suitable kinetic model, rate determining step, and solute uptake phenomenon, we have applied experimental data to all basic kinetic models. The findings from experiments have been analyzed using a variety of kinetic models, including zero-order, first-order, second-order, third-order, pseudo-first-order, and pseudo-second-order models. The correlation co-efficient led to the conclusion that the current readings suited the pseudo-second-order model nicely compared to others, as shown in Fig. 11. q_e is the equilibrium amount of lead adsorbed (mg/g) in this instance. The amount of lead that has been adsorbed at time t (min) is symbolized by the abbreviation q_t (mg/g), and the rate constants for the pseudo-first-order and pseudo-second-order kinetic equations are k_1 and k_2, respectively, in mg min g^{-1}. With a correlation coefficient of 0.985, the experimental data satisfies a pseudo-second-order model (Yadav et al., 2022). Table 3 presents the kinetic parameters of Pb^{2+} adsorption. This suggests that the chemical interactions between Pb^{+2} and the adsorbent determine the rate of chemisorption (Yadav et al., 2019).

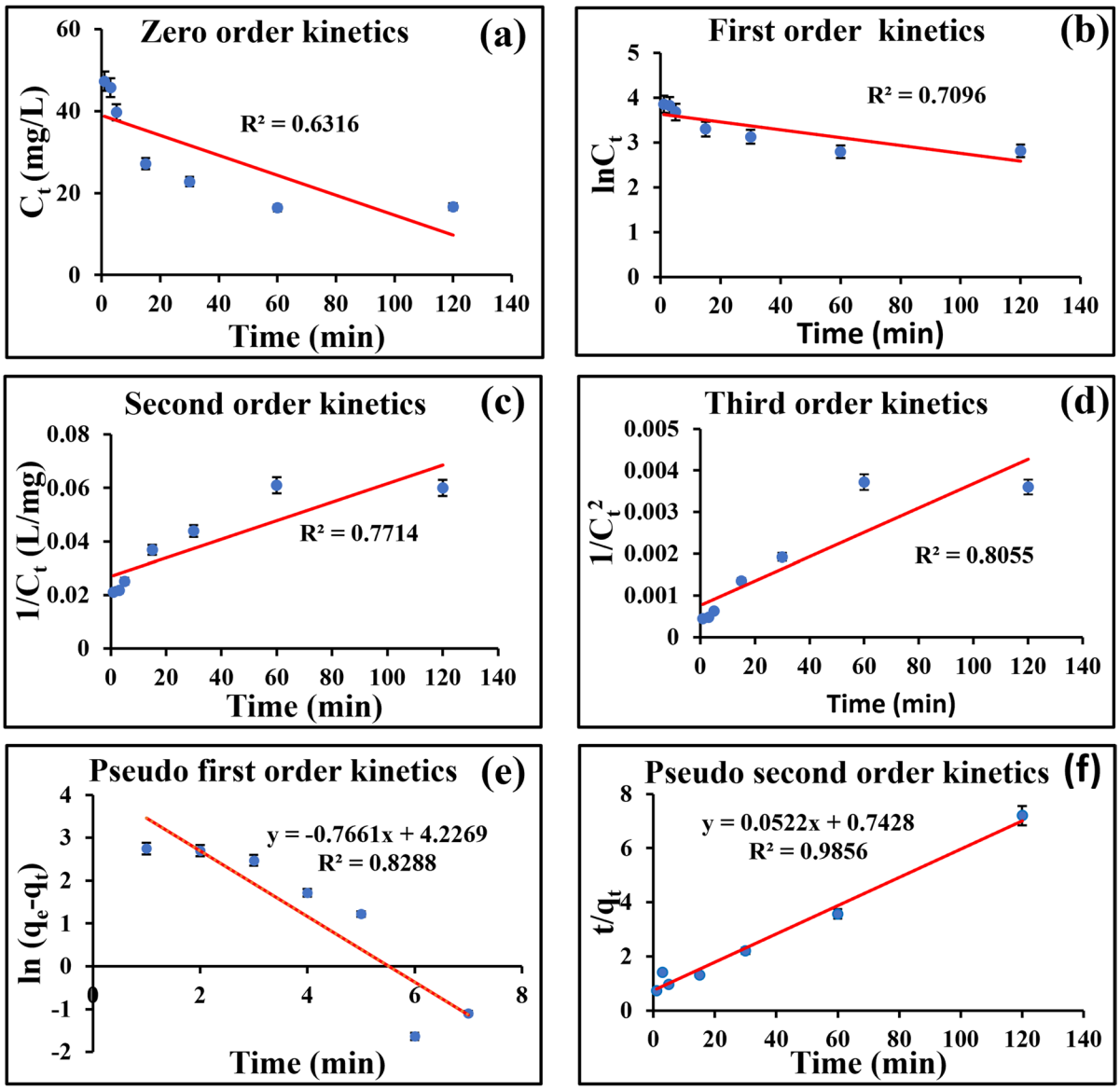

Fig. 11 **a** Zero-order, **b** first-order, **c** second-order, **d** third-order, **e** pseudo first-order, **f** pseudo-second-order kinetic curves for adsorption of Pb^{+2} on SiNP-L_3

Table 3 Coefficients of pseudo-first-order and pseudo-second-order kinetic models for adsorption

Pseudo-first-order kinetics			Pseudo-second-order kinetics		
q_e (mg g^{-1})	K_1 (min^{-1})	R^2	q_e (mg g^{-1})	K_2 (10^{-2} g mg^{-1} min^{-1})	R^2
29.74	0.76	0.828	19.15	0.366	0.985

3.4.5 Adsorption Isotherms

Isotherm is a vital element feature in the procedure of adsorption. Typically, the performance of an adsorbent is estimated using the adsorption isotherm which depends on adsorption equilibrium. At constant temperature, the isotherm for adsorption is defined via the connection between the optimal adsorption concentration (C_e) and the equilibrium rate of adsorption

per gram of mass (q_e) (Hu et al., 2017). The variable is determined by the bulk content and the pollutant that has been adsorbed at the interface. Adsorption isotherms provide a comprehensive description of the nature of interaction and are essential for developing an adsorption system. Pb^{2+} adsorption capacities onto SiNP-L_3 were examined in this context employing Langmuir (Eq. 1) and Freundlich (Eq. 2) isotherm models for adsorption (Fig. 12).

$$\frac{C_e}{q_e} = \frac{1}{K_L} + \frac{C_e}{q_m} \tag{1}$$

$$\log q_e = \log K_F + \frac{1}{n} \log C_e \tag{2}$$

wherein C_e (mg L^{-1}) is the Pb (II) equilibrium amount, the potential for adsorption of Pb (II) at a state of equilibrium is defined by q_e (mg g^{-1}); the highest potential for adsorption (mg g^{-1}) is symbolized by q_m, $1/n$ is a constant affiliated with the adsorption intensity fluctuation owing to adsorbent heterogeneity, and the Langmuir and Freundlich retention constants at equilibrium are denoted by K_L (L/mg) and K_F (L/mg), respectively. Under the conditions of $0<K_L<1$, $K_L>1$, and $K_L=1$, respectively, the value of K_L reflects whether the adsorption is favorable, unfavorable, or linear in nature (Das et al., 2020). Table 4 displays the computed data from the Langmuir and Freundlich equilibrium models. Both adsorption isotherm models accurately predicted the experimental results. The Langmuir model, on the other hand, outperforms the Freundlich model based on the coefficient of correlation, confirming a monolayer adsorption process. In the monolayer formation, specific homogeneous areas on the exterior of adsorbent enhance the adsorption; all of these areas are similar in terms of energy, and no adsorbate molecule migration takes place on the surface's plane (Yadav et al., 2022).

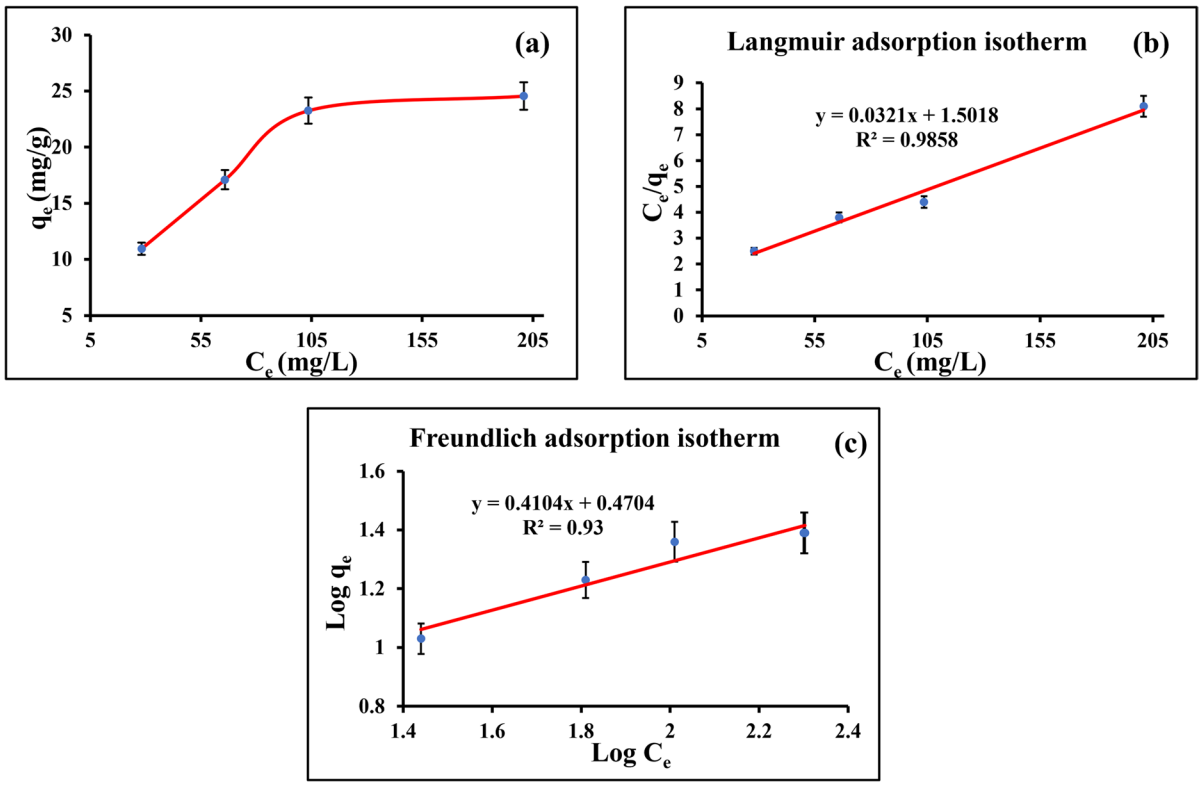

Fig. 12 **a**, **b** Langmuir and **c** Freundlich coefficients of adsorption for Pb^{+2} deposition on SiNP-L_3

Table 4 Coefficients of Langmuir and Freundlich isotherms

Langmuir				Freundlich		
q_m (mg g^{-1})	K_L (L mg^{-1})	R^2	R_L	1/*n*	K_F (L mg^{-1})	R^2
31.15	0.021	0.985	0.935	0.410	1.6	0.93

3.4.6 Thermodynamic Study

The thermodynamics of adsorption is an important technique for determining whether an adsorption response is natural or not. Adsorption mechanism is also determined by the thermodynamic study. Thermodynamic algorithms were employed for estimating the data gathered during adsorption investigations at different temperatures, notably 35 °C, 45 °C, and 55 °C. Several parameters, comprising Gibbs free energy (ΔG°), alteration of entropy (ΔS°), and variation in enthalpy (ΔH°), were computed from the thermodynamic equilibrium parameter (K_c) using the following equations:

$$K_c = \frac{a_s}{a_e} = \frac{\vartheta_s}{\vartheta_e}\frac{q_e}{C_e} \tag{3}$$

Here, the movement of the Pb^{+2} ions tied on the surface of the adsorbent is signified by a_s and its equilibrium activity contained within the solution is symbolized by a_e. The activity factor of adsorbate taken up in solution is signified by ϑs, while the activity factor of adsorbate molecules at equilibrium is signified by ϑe. Whenever the concentration of the adsorbate solution falls and approaches zero, the activity coefficient ϑ eventually hits unity. In such a scenario, the aforementioned equation could be expressed as follows;

$$\lim_{C_e \to 0} \frac{a_s}{a_e} = \frac{q_e}{C_e} = K_c \tag{4}$$

The intercept and slope of a Van't Hof plot of data obtained from experiments ($\ln K_c$ vs 1/T) at a trio of temperatures, 308 K, 318 K, and 328 K, were taken into account to figure out the values of ΔH° and ΔS°. Then, implementing Eq. 5, the Gibbs free energy was computed.

$$\Delta G^0 = -RT \ln K_c \tag{5}$$

$$\ln K_c = \frac{\Delta S^0}{R} - \frac{\Delta H^0}{R}\frac{1}{T} \tag{6}$$

The negative numbers of ΔG° at varying temperatures highlight the natural pattern of Pb^{2+} adhesion on SiNP-L_3. Higher negative numbers with increasing temperature suggest a more energy-efficient technique for adsorption. An increment in the negative numbers of ΔG° at elevated temperature is revealed by the present study as shown in Table 5. The positive value of ΔS° implies a rise in randomness through the adsorption process at the solid-solution junction. A positive reading of ΔH° explains the endothermic character of the adsorption procedure employing adsorbent SiNP-L_3. Furthermore, the physisorption mechanism is illustrated by ΔH° values that span 2.1–20.9 kJ mol^{-1}, and the chemisorption technique is outlined by values spanning from 80–200 kJ mol^{-1}. Because the results of the computation exceed 20.9, chemisorption is accompanied by SiNP-L_3 for extraction of Pb (II). This validates the kinetics modeling that had been identified (Yadav et al., 2022).

3.4.7 Desorption Study

To make the practice of adsorption economical and profitable, the adsorbent must have properties such as greater capacity to adsorb, easy renewal, and replicated reuse abilities. The desorption study is a vital indicator for renewing the adsorbent and recuperating the Pb^{+2} ions. The efficiency of the adsorbent is also explained by the desorption

Table 5 Thermodynamic parameters for the adsorption of Pb^{+2} on SiNP-L_3

Temperature (K)	K_c	ΔG^0(kJ mol^{-1})	ΔH^0 (kJ mol^{-1})	ΔS^0 (J K^{-1} mol^{-1})
308	1.14	−346.14	31.16	102.19
318	1.60	−1244.01		
328	2.40	−2395.31		

experiments. For the act of desorption to be successful, a compatible solvent arrangement that corresponds to the characteristics of adsorbent and adsorbate interplay is required (Yadav et al., 2022). To explore the reusability of SiNP-L_3, repeated adsorption/desorption rounds have been conducted with 0.01N, 0.1N, 2N, and 6N HCl and 0.01N, 0.1N NaOH as eluents (Fig. 13a). The outcomes establish that 2N HCl (5-10 ml per g of support followed by washing with deionized water) is a more beneficial desorption eluent rather than NaOH. The rapid desorption efficiency with 2N HCl could be attributed to the robust relationship of Pb (II) ions with the external functionalities present on the SiNP-L_3 adsorbent, boosting desorption. Ninety-eight percent of extraction efficiency was found with 2N HCl as eluent (Tighadouini et al., 2021). Results indicate that extraction efficiency gradually declines after each cycle (Fig. 13b). The characteristic spectra of SiNP-L_3 after regeneration are preserved as suggested by FT-IR investigation, as shown in Fig. 13c. This implies that SiNP-L_3 preserves its structure after effective Pb^{2+} adsorption, increasing the economic feasibility of the process (Radi et al., 2016; Tighadouini et al., 2017).

3.4.8 *Effect of Coexisting Ions*

Several more common metal ions (Li(I), Na(I), K(I), Ca (II), Mg (II), Cd II), Cr (III), Cu (II), Ni (II), and Zn (II)) in aqueous solution were utilized to conduct studies for Pb (II) selectivity. At pH 5, 100 mg of SiNP-L_3 was added to 50 mL of a watery solution containing about 50 mg/L of each of the metal ions claimed before. The adsorption fraction of the Pb (II) ions on the SiNP-L_3 approached over 85%, while lower than 15% other metal ions in which is not affected by the presence of large excess of several common alkali and alkaline earth metal ions (see Fig. 14). This illustrates that SiNP-L_3 remains capable to capture Pb (II) ions in almost measurable concentrations even when multiple competing metal ions are present in solution, making SiNP-L_3 a perfect option for selective lead adsorption. We assumed that the differing affinities between SiNP-L_3 and Pb (II) ions or other metal ions were

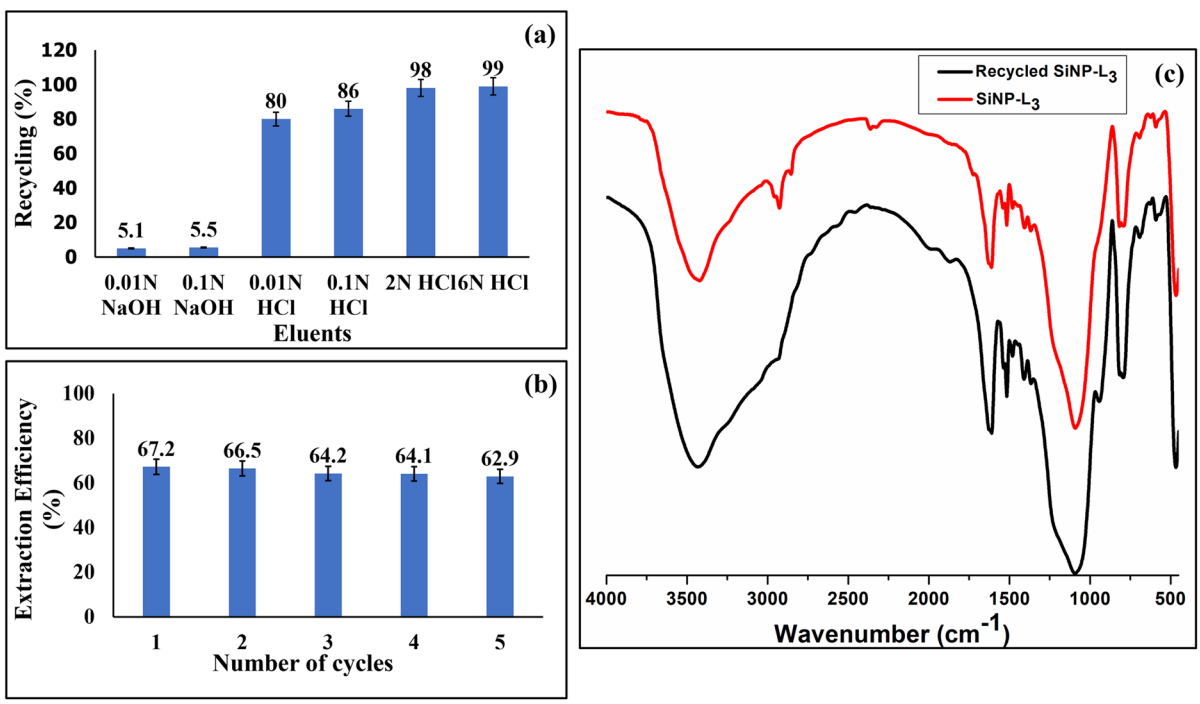

Fig. 13 **a** Screening of various eluents for recycling, **c** FT-IR spectra comparison of SiNP-L_3 with recycled SiNP-L_3, **b** extraction efficiency after every adsorption-desorption cycle using 2N HCl as eluent

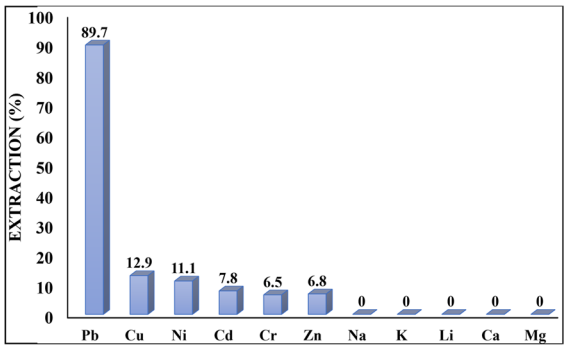

Fig. 14 Selectivity for Pb (II) in the presence of other metal ions

the cause of the adsorption selectivity of SiNP-L_3 for Pb (II) ions. As a result, we inquired about the previously reported data about the electronegativity and ionic diameter values of metal ions, as shown in Table 6 (Li et al., 2015). Pb (II) has the next biggest ionic radius, while a variety of metal ions have considerably fewer radii than it. In summary, a robust steric barrier preventing extra metal ions from physically reaching the adsorption sites appeared unlikely to exist. Fortunately, Pb (II) ions exhibited the highest absolute electronegativity of any other metal ion used in this investigation, indicating that Pb (II) has the strongest attraction to the isolated pairs of electrons on oxygen and nitrogen atoms and can thus form extremely resilient complexes. Owing to the hypothesis of hard and soft acids and bases (HSAB), Schiff ligands operate as Lewis soft bases, while Pb (II) ions may be designated a middle-soft acid. As a result of the attraction of electrostatic charge and chelating interaction, the significant affection of SiNP-L_3 toward the desired Pb (II) could be observed (Zheng et al., 2021). These two are probably what caused Pb (II) ions to preferentially bind to SiNP-L_3 over other metal ions. Additionally, it has been determined that practically all metal ions have absolute electronegativity values lower than Pb (II) ions; therefore, this would not be a barrier to the use of SiNP-L_3 for the selective capturing of Pb (II) ions in real water samples.

3.4.9 Adsorption Mechanism

The probable interaction of SiNP-L_3 with Pb^{2+} is shown in Fig. 15. The pore volume, surface area, active sites, and surface chemical groups of the adsorbent, as well as the structural and functional behavior of the adsorbate molecules, all influence the adsorption mechanism (Zhou et al., 2019). Cationic pollutant is involved in this system, i.e., heavy metal (Pb^{2+}). Host-guest interaction is initially thought to be the process of adsorption dependent on significant selectivity for Pb^{+2} ions. The adsorbate molecules get attracted to the oxygen and nitrogen donor atoms where they form six-member chelation rings with their lone pair of electrons. The number of active sites and the microstructure of the adsorbent have an impact on both the adsorption capacity and the rate of adsorption. Therefore, it is believed that Pb (II) adsorption involves electrostatic interaction (Al-Wasidi et al., 2022b; Tighadouini et al., 2017).

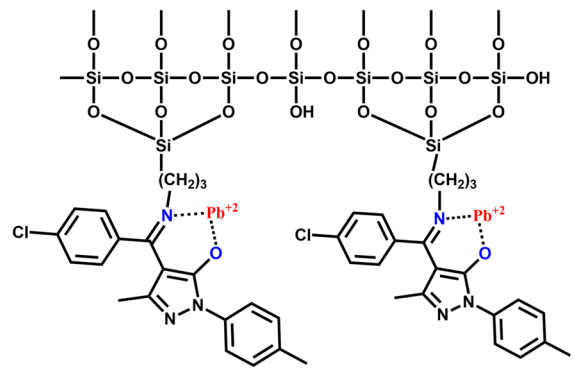

Fig. 15 Probable adsorption mechanism for SiNP-L_3

Table 6 Physical characteristics of several metal ions

Parameters	Metal ions									
	Li(I)	Na(I)	K(I)	Ca(II)	Mg(II)	Pb(II)	Cd(II)	Cr(III)	Ni(II)	Zn(II)
Ionic radius (A^0)	0.076	0.102	0.138	0.100	0.072	0.119	0.095	0.062	0.069	0.074
Absolute electronegativity	1.00	0.93	0.82	1.00	1.31	2.33	1.69	1.66	1.92	1.65

3.4.10 Comparison with Alternate Adsorbents (Table 7)

4 Conclusion

In this study, novel silica functionalized with acyl pyrazolone Schiff base ligand (L_3) was successfully prepared. 3-Aminopropyl trimethoxy silane was used to initially modify the surface of the activated silica gel through a reaction with exterior silanol groups and then simple Schiff base reaction with (4-chlorophenyl) [5-hydroxy-3-methyl-1-(4-methylphenyl)-1*H*-pyrazol-4-yl] methanone was carried out to prepare introduced sorbent SiNP-L_3. The new material was well characterized by scanning electron microscopy, the Fourier transformation of infrared spectroscopy, elemental examination, BET surface measurement, Barrett-Joyner-Halenda pore dimension, solid-state ^{13}C-NMR, powder XRD, and thermogravimetry measurements. The newly synthesized eco-friendly adsorbent displayed good thermal stability and selective adsorption capacity from aqueous solutions towards Pb (II) ions. The adsorption isotherms of Pb (II) fitted well with the Langmuir Isotherm Model (R^2=0.98), indicating that the adsorption mechanism followed Langmuir monolayer adsorption, and the adsorption kinetics of Pb (II) followed the pseudo-second-order kinetic model (R^2=0.98). In addition, the newly synthesized material was proven to be a cost-effective adsorbent and could be used for the selective extraction of Pb (II) from contaminated water even in the presence of other metal ions having an adsorption capacity of 16.8 mg g^{-1}. Also, as the adsorption process of Pb (II) on a synthetic adsorbent SiNP-L_3 is endothermic, we may consider optimizing the conditions for large-scale experiments. According to Le Chatelier's principle, in endothermic processes, if we increase the temperature, the reaction rate (here extraction rate) also increases. So we can increase the temperature up to 65°C (as we have done in thermodynamic study) as water is the solvent. Also, during adsorption, we have to use efficient insulation to minimize heat loss and explore ways to enhance the kinetics of the endothermic process. Additionally,

Table 7 Comparison study of present work with previously reported literatures

Adsorbent	Pb^{+2} adsorption capacity (mg g^{-1})	Reference
Support: Silica (SiO_2)		
2,3-Dihydroxy benzaldehyde (N, O donor)	3.33	(Koorepazan Moftakhar et al., 2016)
4-Amino, 2-mercapto Pyrimidine	2.07	(De Oliveira et al., 2015)
Resacetophenone	13.80	(Goswami & Singh, 2002)
4-Amino-5-hydrazino-1,2,4-triazole-3-thiol	14.49	(Ivassechen et al., 2018)
Acid red-88	3.35	(Kocjan, 1999)
TiO_2 nanoparticles	3.16	(R. Liu & Liang, 2008)
Pyrazole derivatives	9.2	(Radi et al., 2003)
Thiophene (S-donor)	11.3	(Radi & Attayibat, 2010)
Gallic acid	12.63	(Xie et al., 2008)
Dithizone	8.28	(Zaporozhets et al., 1999)
Multi-amine donors (N donor)	1.1	(Zhang et al., 2007)
Present work Acyl pyrazolone ligand (L_3) (N, O donor)	**16.8**	-
Other materials		
Activated carbon-alginate	15.7	(Cataldo et al., 2016)
Iron-coated Australian zeolite	11.2	(Nguyen et al., 2015)
2-Mercaptobenzothiazole supported on TiO_2 nanoparticles	3.17	(Pourreza et al., 2014)

monitoring other factors such as pH, concentration, and contact time is crucial for successful large-scale implementation.

Acknowledgements The authors are thankful to the DST-INSPIRE Fellowship, Government of India, New Delhi, India. The authors acknowledge the Department of Environmental Science for the AAS facility, the Department of Applied Physics for Powder-XRD analysis, the Department of Geology for SEM analysis, the Department of Chemistry, MSU, Baroda, and Sud-Chemie India Private Limited, Vadodara, India, for BET surface area and BJH pore size measurements. Special thanks to Dr. Monika Yadav for her constant support and guidance regarding application work.

Author Contribution Both the authors contributed to the study conception and design. Material preparation, data collection, and analysis were performed by PK. The first draft of the manuscript was written by PK. *RNJ* has read and approved the final manuscript.

Funding *This work was supported by the DST-INSPIRE Fellowship (Application Reference No.* DST/INSPIRE/03/2022/004114 *and Fellowship award No. I*F210568). *Author P.K. has received research support from the Department of Science and Technology, Government of India, New Delhi, India.*

Data Availability The authors declare that the data supporting the findings of this study are available within the paper and its Supplementary Information files. Should any raw data files be needed in another format, they are available from the corresponding author upon reasonable request.

Declarations

Ethical Approval Not applicable

Consent to Participate Both the authors agreed to participate in this work.

Consent for Publication Both the authors agreed to publish this work in Water, Air, & Soil Pollution.

Competing Interests The authors declare no competing interests.

References

El Abiad, C., Radi, S., El, M. M., Lamsayah, M., Figueira, F., Amparo, M., Faustino, F., Graça, M., Neves, P. M. S., & Moura, N. M. M. (2017). Porphyrin-silica gel hybrids as effective and selective copper (II) adsorbents from wastewater. *Journal of Hazardous Materials, 370*, 80–90. https://doi.org/10.1016/j.jhazmat.2017.10.058

Ahmed, M. O., Shrpip, A., & Mansoor, M. (2020). Synthesis and characterization of new Schiff base/thiol-functionalized mesoporous silica: An efficient sorbent for the removal of Pb (II) from aqueous solutions. *Processes, 8*(2), 246. https://doi.org/10.3390/pr8020246

Al-Wasidi, A. S., Naglah, A. M., Saad, F. A., & Abdelrahman, E. A. (2022a). Modification of silica nanoparticles with 1-hydroxy-2-acetonaphthone as a novel composite for the efficient removal of Ni (II), Cu (II), Zn (II), and Hg (II) ions from aqueous media. *Arabian Journal of Chemistry, 15*, 104010. https://doi.org/10.1016/j.arabjc.2022.104010

Al-Wasidi, A. S., Naglah, A. M., Saad, F. A., & Abdelrahman, E. A. (2022b). Modification of silica nanoparticles with 4,6-diacetylresorcinol as a novel composite for the efficient removal of Pb (II), Cu (II), Co (II), and Ni (II) ions from aqueous media. *Journal of Inorganic and Organometallic Polymers and Materials, 32*, 2332–2344. https://doi.org/10.1007/s10904-022-02282-4

Amarasekara, A. S., Owereh, O. S., & Aghara, S. K. (2009a). Synthesis of 4-acylpyrazolone Schiff base ligand grafted silica and selectivity in adsorption of lanthanides from aqueous solutions. *Journal of Rare Earths, 27*(5), 870–874. https://doi.org/10.1016/S1002-0721(08)60352-X

Amarasekara, A. S., Owereh, O. S., & Aghara, S. K. (2009b). Synthesis of functionalized polysiloxane 4-acylpyrazolone Schiff base ligand system and its applications in the adsorption of lanthanide ions from aqueous solutions. *Journal of Sol-Gel Science and Technology, 52*(3), 382–387. https://doi.org/10.1007/s10971-009-2041-z

Atia, A. A., Donia, A. M., & Elwakeel, K. Z. (2005). Selective separation of mercury (II) using a synthetic resin containing amine and mercaptan as chelating groups. *Reactive and Functional Polymers, 65*(3), 267–275. https://doi.org/10.1016/j.reactfunctpolym.2005.07.001

Bacalum, E., Radulescu, M., Iorgulescu, E.-E., & David, V. (2011). breakthrough parameters of SPE procedure on C18 cartridges for some polar compounds. *Revue Roumaine de Chimie, 56*(2), 137–143.

Bessbousse, H., Rhlalou, T., Verchère, J. F., & Lebrun, L. (2008). Sorption and filtration of Hg (II) ions from aqueous solutions with a membrane containing poly(ethyleneimine) as a complexing polymer. *Journal of Membrane Science, 325*(2), 997–1006. https://doi.org/10.1016/j.memsci.2008.09.035

Cataldo, S., Gianguzza, A., Milea, D., Muratore, N., & Pettignano, A. (2016). Pb (II) adsorption by a novel activated carbon – alginate composite material. A kinetic and equilibrium study. *International Journal of Biological Macromolecules, 92*, 769–778. https://doi.org/10.1016/j.ijbiomac.2016.07.099

Das, M., Yadav, M., Shukla, F., Ansari, S., Jadeja, R. N., & Thakore, S. (2020). Facile design of a dextran derived polyurethane hydrogel and metallopolymer: A sustainable approach for elimination of organic dyes and reduction of nitrophenols. *New Journal of Chemistry, 44*, 19122–19134. https://doi.org/10.1039/d0nj01871f

De Oliveira, J. A., Pereira, S. P., Da Silva, R. I. V., Saeki, M. J., Martines, M. A. U., De Albuquerque, P. V., & De Castro, G. R. (2015). Application of mesoporous SBA-15 silica functionalized with 4-amino-2-mercaptopyrimidine for the adsorption of Cu (II), Zn (II), Cd (II), Ni (II), and Pb

(II) from water. *Acta Chimica Slovenica, 62*(1), 111–121. https://doi.org/10.17344/acsi.2014.787

George, A., & Stephen Brunauer, B. (1938). adsorption of gases in multimolecular layers. *J Ame Che Soc, 60*(2), 309–319. https://doi.org/10.1021/ja01269a023

Goswami A, Singh AK (2002) Silica gel functionalized with resacetophenone: Synthesis of a new chelating matrix and its application as metal ion collector for their flame atomic absorption spectrometric determination. Analytica Chimica Acta 454(2):229-240. http://dx.doi.org/https://doi.org/10.1016/S0003-2670(01)01552-5

Han, D. M., Fang, G. Z., & Yan, X. P. (2005). Preparation and evaluation of a molecularly imprinted sol-gel material for on-line solid-phase extraction coupled with high performance liquid chromatography for the determination of trace pentachlorophenol in water samples. *Journal of Chromatography. A, 1100*(2), 131–136. https://doi.org/10.1016/j.chroma.2005.09.035

Hu, C., Zhu, P., Cai, M., Hu, H., & Fu, Q. (2017). Comparative adsorption of Pb (II), Cu (II) and Cd (II) on chitosan saturated montmorillonite: Kinetic, thermodynamic and equilibrium studies. *Applied Clay Science, 143*, 320–326. https://doi.org/10.1016/j.clay.2017.04.005

Irfan, D., Tang, X., Abdulhasanb, M. J., Zaidi, M., Mustafa, Y. F., Jasem, H., Altimari, U. S., & Chem, C. (2022). Epichlorohydrin crosslinked 2,4-dihydroxybenzaldehyde Schiff base chitosan@SrFe12O19 (EP-DBSB-CS@SrFe12O19) Magnetic nanocomposite for efficient removal of Pb (II) and Cd (II) from aqueous solution. *Journal of Polymers and the Environment, 30*(10), 1–9. https://doi.org/10.1007/s10924-022-02505-2

Ivassechen, J., Rócio, D., Jorgetto, A. D. O., Wondracek, M. H., Silva, A. C. P. D., Zara, L. F., et al. (2018). Adsorptive properties of mesoporous silica modified with Lewis base molecule and its application in the preconcentration of Cu (II), Co (II), and Cd (II) from aqueous media. *Turkish Journal of Chemistry, 42*(2), 547–561. https://doi.org/10.3906/kim-1709-43

Jensen, B. S. (1959). The synthesis of 1-phenyl-3-methyl-4-acyl-pyrazolones-5. *Acta Chemica Scandinavica, 13*(8), 1668–1670.

Jiang, Y., Gao, Q., Yu, H., Chen, Y., & Deng, F. (2007). Intensively competitive adsorption for heavy metal ions by PAMAM-SBA-15 and EDTA-PAMAM-SBA-15 inorganic-organic hybrid materials. *Microporous and Mesoporous Materials, 103*(1-3), 316–324. https://doi.org/10.1016/j.micromeso.2007.02.024

Kocjan, R. (1999). Retention of some metal ions and their separation on silica gel modified with acid Red 88. *Microchimica Acta, 131*, 153–158. https://doi.org/10.1007/s006040050021

Koorepazan Moftakhar, M., Dousti, Z., Yaftian, M. R., & Ghorbanloo, M. (2016). Investigation of heavy metal ions adsorption behavior of silica-supported Schiff base ligands. *Desalination and Water Treatment, 57*(56), 27396–27408. https://doi.org/10.1080/19443994.2016.1170638

Li, L., Qian, Y., Zhang, H. M., Han, H., & Qiao, P. (2020). Selective adsorption of Pb (II) by a silica gel-immobilized schiff bas. *Desalination and Water Treatment, 174*, 291–300. https://doi.org/10.5004/dwt.2020.24844

Li, X., Wang, Z., Li, Q., Ma, J., & Zhu, M. (2015). Preparation, characterization, and application of mesoporous silica-grafted graphene oxide for highly selective lead adsorption. *Chemical Engineering Journal, 273*, 630–637. https://doi.org/10.1016/j.cej.2015.03.104

Liu, R., & Liang, P. (2008). Determination of trace lead in water samples by graphite furnace atomic absorption spectrometry after preconcentration with nanometer titanium dioxide immobilized on silica gel. *Journal of Hazardous Materials, 152*, 166–171. https://doi.org/10.1016/j.jhazmat.2007.06.081

Low, K. S., Lee, C. K., & Liew, S. C. (2000). Sorption of cadmium and lead from aqueous solutions by spent grain. *Process Biochemistry, 36*(1-2), 59–64. https://doi.org/10.1016/S0032-9592(00)00177-1

Miao, J., Qian, J., Wang, X., Zhang, Y., Yang, H., & He, P. (2009). Synthesis and characterization of ordered mesoporous silica by using polystyrene microemulsion as templates. *Materials Letters, 63*, 989–990. https://doi.org/10.1016/j.matlet.2009.01.065

Mishra, P. C., & Patel, R. K. (2009). Removal of lead and zinc ions from water by low-cost adsorbents. *Journal of Hazardous Materials, 168*, 319–325. https://doi.org/10.1016/j.jhazmat.2009.02.026

Mureseanu, M., Reiss, A., Cioatera, N., Trandafir, I., & Hulea, V. (2010). Mesoporous silica functionalized with 1-furoyl thiourea urea for Hg (II) adsorption from aqueous media. *Journal of Hazardous Materials, 182*, 197–203. https://doi.org/10.1016/j.jhazmat.2010.06.015

Myers, R. T. (1978). Thermodynamics of chelation. *Inorganic Chemistry, 17*(4), 952–958. https://doi.org/10.1021/ic50182a032

Nasu, A., Yamauchi, S., & Sekine, T. (1997). Solvent extraction of copper(I) and (II) as thiocyanate complexes with tetrabutylammonium ions into chloroform and with trioctylphosphine oxide into hexane. *Analytical Sciences, 13*, 903–911. https://doi.org/10.2116/analsci.13.903

Nguyen, T. C., Loganathan, P., Nguyen, T. V., Vigneswaran, S., Kandasamy, J., & Naidu, R. (2015). Simultaneous adsorption of Cd, Cr, Cu, Pb, and Zn by an iron-coated Australian zeolite in batch and fixed-bed column studies. *Chemical Engineering Journal, 270*, 393–404. https://doi.org/10.1016/j.cej.2015.02.047

Pearson, R. G., & Busch, D. H. (1963). Hard and soft acids and bases. *Journal of the American Chemical Society, 85*, 3533–3539. https://doi.org/10.1021/ja00905a001

Pourreza, N., Rastegarzadeh, S., & Larki, A. (2014). Simultaneous preconcentration of Cd (II), Cu (II) and Pb (II) on Nano-TiO2 modified with 2-mercaptobenzothiazole prior to flame atomic absorption spectrometric determination. *Journal of Industrial and Engineering Chemistry, 20*, 2680–2686. https://doi.org/10.1016/j.jiec.2013.10.055

Pratiwi, D., Saprudin, D., & Rohaeti, E. (2017). Synthesis of activated carbon-nanomagnetite-pyrazolone(1-phenyl-3-methyl-5-pyrazolone) composite as adsorbent for Cd^{2+}. *IOP Conference Series: Earth and Environmental Science, 58*, 012003. https://doi.org/10.1088/1755-1315/58/1/012003

Price, P. M., Clark, J. H., & Macquarrie, D. J. (2000). Modified silicas for clean technology. *Journal of the Chemical*

Society, Dalton Transactions, 101–110. https://doi.org/10.1039/a905457j

Radi, S., El, A. C., Moura, N. M. M., Faustino, M. A. F., & Neves, M. G. P. M. S. (2019). New hybrid adsorbent based on porphyrin functionalized silica for heavy metals removal: Synthesis, characterization, isotherms, kinetics and thermodynamics studies. *Journal of Hazardous Materials, 80–90*. https://doi.org/10.1016/j.jhazmat.2017.10.058

Radi, S., & Attayibat, A. (2010). Functionalized SiO_2 with S-donor thiophene: Synthesis, characterization, and its heavy metals adsorption. *Phosphorus, Sulfur and Silicon and the Related Elements, 185*, 2003–2013. https://doi.org/10.1080/10426500903440042

Radi, S., Basbas, N., Tighadouini, S., Bacquet, M., Degoutin, S. P., & Cazier, F. (2013). New amine-modified silicas: synthesis, characterization and its use in the Cu (II)-removal from aqueous solutions. *Progress in Nanotechnology and Nanomaterials, 2*(4), 108–116. https://doi.org/10.5963/PNN0204002

Radi, S., El Abiad, C., Carvalho, A. P., Santos, S. M., Faustino, M. A. F., Neves, M. G. P. M. S., & Moura, N. M. M. (2018). An efficient hybrid adsorbent based on silica-supported amino penta-carboxylic acid for water purification. *Journal of Materials Chemistry A, 6*, 13096–13109. https://doi.org/10.1039/c8ta02560f

Radi, S., Ramdani, A., Lekchiri, Y., Morcellet, M., Crini, G., Janus, L., & Bacquet, M. (2003). Immobilization of pyrazole compounds on silica gels and their preliminary use in metal ion extraction. *New Journal of Chemistry, 27*, 1224–1227. https://doi.org/10.1039/b301111a

Radi, S., Tighadouini, S., Bacquet, M., Degoutin, S., Cazier, F., Zaghrioui, M., & Mabkhot, Y. N. (2014). Organically modified silica with pyrazole-3-carbaldehyde as a new sorbent for solid-liquid extraction of heavy metals. *Molecules, 19*, 247–262. https://doi.org/10.3390/molecules19010247

Radi, S., Toubi, Y., El-Massaoudi, M., Bacquet, M., Degoutin, S., & Mabkhot, Y. N. (2016). Efficient extraction of heavy metals from aqueous solution by novel hybrid material based on silica particles bearing new Schiff base receptor. *Journal of Molecular Liquids, 223*, 112–118. https://doi.org/10.1016/j.molliq.2016.08.024

Roumeliotis, P., Kurganov, A. A., & Davankov, V. A. (1983). Effect of the hydrophobic spacer in bonded [cu(l-hydroxyprolyl)alkyl]$^+$ silicas on retention and enantioselectivity of (a-amino acids in high-performance liquid chromatography). *Journal of Chromatography A, 266*, 439–450. https://doi.org/10.1016/S0021-9673(01)90915-X

Sales, J. A. A., & Airoldi, C. (2005). Calorimetric investigation of metal ion adsorption on 3- glycidoxypropyltrimethylsiloxane + propane-1,3-diamine immobilized on silica gel. *Thermochimica Acta, 427*, 77–83. https://doi.org/10.1016/j.tca.2004.08.015

Shaikh, I., Jadeja, R. N., & Patel, R. (2020). Three mixed ligand mononuclear Zn (II) complexes of 4-acyl pyrazolones: Synthesis, characterization, crystal study and antimalarial activity. *Polyhedron, 183*, 114528. https://doi.org/10.1016/j.poly.2020.114528

Shaikh, I., Jadeja, R. N., Patel, R., Mevada, V., & Gupta, V. K. (2021). 4-acylhydrazone-5-pyrazolones and their zinc (II) metal complexes: Synthesis, characterization, crystal feature and antimalarial activity. *Journal of Molecular Structure, 1232*, 130051. https://doi.org/10.1016/j.molstruc.2021.130051

Sing, K. S. W., & Williams, R. T. (2004). Physisorption hysteresis loops and the characterization of nanoporous materials. *Adsorption Science and Technology, 22*(10), 773–782. https://doi.org/10.1260/0263617053499032

Song, Q., Cheng, M., Liu, H., Jia, H., Nan, Y., Zheng, W., Li, Y., & Bao, J. J. (2023). Preparation of a phenylboronic acid and aldehyde bi-functional group modified silica absorbent and applications in removing Cr (VI) and reducing to Cr (III). *RSC Advances, 13*, 15554–15565. https://doi.org/10.1039/d3ra02009f

Soylak, M., & Erdogan, N. D. (2006). Copper (II)-rubeanic acid coprecipitation system for separation-preconcentration of trace metal ions in environmental samples for their flame atomic absorption spectrometric determinations. *Journal of Hazardous Materials, 137*, 1035–1041. https://doi.org/10.1016/j.jhazmat.2006.03.031

Tao G, Fang Z (1998) Dual stage preconcentration system for flame atomic absorption spectrometry using flow injection on-line ion-exchange followed by solvent extraction. Fresenius J Anal Chem 360:156–160. https://doi.org/10.1007/s002160050667

Tighadouini, S., Radi, S., Bacquet, M., Degoutin, S., Zaghrioui, M., Jodeh, S., & Warad, I. (2017). Removal efficiency of Pb (II), Zn (II), Cd (II) and Cu (II) from aqueous solution and natural water by ketoenol–pyrazole receptor functionalized silica hybrid adsorbent. *Separation Science and Technology (Philadelphia), 52*, 608–621. https://doi.org/10.1080/01496395.2016.1262874

Tighadouini, S., Roby, O., Radi, S., Lakbaibi, Z., Saddik, R., Mabkhot, Y. N., Almarhoon, Z. M., & Garcia, Y. (2021). A highly efficient environmental-friendly adsorbent based on schiff base for removal of Cu (II) from aqueous solutions: A combined experimental and theoretical study. *Molecules, 26*(17), 5164. https://doi.org/10.3390/molecules26175164

Tong Akama, Y., & Tanaka, S. (1990). Preconcentration of indium with l-phenyl-3-methyl-4-stearoyl-5-pyrazolone on silica gel. *Analytica Chimica Acta, 230*, 175–177. https://doi.org/10.1016/S0003-2670(00)82777-4

Xie, F., Lin, X., Wu, X., & Xie, Z. (2008). Solid phase extraction of lead (II), copper (II), cadmium (II) and nickel (II) using gallic acid-modified silica gel prior to determination by flame atomic absorption spectrometry. *Talanta, 74*, 836–843. https://doi.org/10.1016/j.talanta.2007.07.018

Yadav, M., Das, M., Savani, C., Thakore, S., & Jadeja, R. (2019). Maleic anhydride cross-linked β-cyclodextrin-conjugated magnetic nanoadsorbent: An ecofriendly approach for simultaneous adsorption of hydrophilic and hydrophobic dyes. *ACS Omega, 4*, 11993–12003. https://doi.org/10.1021/acsomega.9b00881

Yadav, M., Jadeja, R., & Thakore, S. (2022). An ecofriendly approach for methylene blue and lead (II) adsorption onto functionalized Citrus limetta Bioadsorbent. *Environmental Processes, 9*(2), 27. https://doi.org/10.1007/s40710-022-00583-x

Zaporozhets, O., Petruniock, N., & Sukhan, V. (1999). Determination of Ag(I), Hg (II) and Pb (II) by using silica gel

loaded with dithizone and zinc dithizonate. *Talanta, 50*(4), 865–873. https://doi.org/10.1016/s0039-9140(99)00172-1

Zhang, L., Chang, X., Hu, Z., Zhang, L., Shi, J., & Gao, R. (2010). Selective solid phase extraction and preconcentration of mercury (II) from environmental and biological samples using nanometer silica functionalized by 2,6-pyridine dicarboxylic acid. *Microchimica Acta, 168*, 79–85. https://doi.org/10.1007/s00604-009-0261-0

Zhang, L., Yu, C., Zhao, W., Hua, Z., Chen, H., Li, L., & Shi, J. (2007). Preparation of multi-amine-grafted mesoporous silicas and their application to heavy metal ions adsorption. *Journal of Non-Crystalline Solids, 353*, 4055–4061. https://doi.org/10.1016/j.jnoncrysol.2007.06.018

Zheng, L., Yang, Y., Zhang, Y., Zhu, T., & Wang, X. (2021). Functionalization of SBA-15 mesoporous silica with bis-schiff base for the selective removal of Pb (II) from water. *Journal of Solid State Chemistry, 301*, 122320. https://doi.org/10.1016/j.jssc.2021.122320

Zhou, Y., Cao, S., Xi, C., Li, X., Zhang, L., Wang, G., & Chen, Z. (2019). A novel Fe3O4/graphene oxide/citrus peel-derived bio-char based nanocomposite with enhanced adsorption affinity and sensitivity of ciprofloxacin and sparfloxacin. *Bioresource Technology, 292*, 121951. https://doi.org/10.1016/j.biortech.2019.121951